Journal of Geoscience and Environment Protection, 2018, 6, 1-21
http://www.scirp.org/journal/gep
ISSN Online: 2327-4344
ISSN Print: 2327-4336

Characterisation of Fractures and Fracture Zones in a Carbonate Aquifer Using Electrical Resistivity Tomography and Pricking Probe Methodes

Sándor Szalai[1*], Attila Kovács[2], Lukács Kuslits[1], Gábor Facskó[1], Katalin Gribovszki[1], János Kalmár[1], László Szarka[1]

[1]MTA CSFK GGI, Sopron, Hungary
[2]MTA-ME Geoengineering Research Group, Budapest, Hungary
Email: *szalai@ggki.hu

How to cite this paper: Szalai, S., Kovács, A., Kuslits, L., Facskó, G., Gribovszki, K., Kalmár, J. and Szarka, L. (2018) Characterisation of Fractures and Fracture Zones in a Carbonate Aquifer Using Electrical Resistivity Tomography and Pricking Probe Methodes. *Journal of Geoscience and Environment Protection*, **6**, 1-21.
https://doi.org/10.4236/gep.2018.64001

Received: December 23, 2017
Accepted: March 6, 2018
Published: March 9, 2018

Abstract

Position, width and fragmentation level of fracture zones and position, significance and characteristic distance of fractures were aimed to determine in a carbonate aquifer. These are fundamental parameters, e.g. in hydrogeological modelling of aquifers, due to their role in subsurface water movements. The description of small scale fracture systems is however a challenging task. In the test area (Kádárta, Bakony Mts, Hungary), two methods proved to be applicable to get reasonable information about the fractures: Electrical Resistivity Tomography (ERT) and Pricking-Probe (PriP). PriP is a simple mechanical tool which has been successfully applied in archaeological investigations. ERT results demonstrated its applicability in this small scale fracture study. PriP proved to be a good verification tool both for fracture zone mapping and detecting fractures, but in certain areas, it produced different results than the ERT. The applicability of this method has therefore to be tested yet, although its problems most probably origin from human activity which reorganises the near-surface debris distribution. In the test site, both methods displayed fracture zones including a very characteristic one and a number of individual fractures and determined their characteristic distance and significance. Both methods prove to be able to produce hydrogeologically important parameters even individually, but their simultaneous application is recommended to decrease the possible discrepancies.

Keywords

Karst, Fracture, Fracture Zone, Electrical Resistivity Tomography, Pricking Probe

1. Introduction

35% of the land surface in Europe is covered by karst according to Karst in Europe COST 65 [1] and 25% of the global population is supplied by drinking water from karst aquifers [2]. These facts underline the importance of studying karst systems. Reference [3] demonstrated the importance of fractures in the development of a classical fracture-dominated karst aquifer. Several hydrogeological conceptual models have been developed for the characterisation of karst systems [4] [5] [6]. These models aim at qualitatively describing the hydrodynamic functioning of karst systems. The conceptual model produced by [7] and [8] provides a quantitative characterisation of karst and fractured systems. In this model, the spatial frequency of karst conduits is one of the crucial parameters influencing the hydraulic functioning of a karst or fractured system. Understanding the hydraulic behaviour of karst systems is important for water research assessment, contamination risk assessment, vulnerability assessment, flood prediction, and speleological studies (e.g. [9] [10]).

Fractures are also important in engineering and geotechnical practice. They affect the stability of engineered structures and excavations [11]. Sinkholes, which develop along conductive underground features, are often responsible for large scale damages in artificial structures, and represent significant engineering issues.

Hydraulically, fractures behave as conductive features; however, in many cases they represent significant hydraulic barriers perpendicular to groundwater flow. Therefore, the identification, localisation and characterisation of fractures are crucial in studying karst and fractured systems.

At the catchment scale, it is possible to identify conduit locations e.g. on basis of sinkhole mapping [12] [13] or by geophysical methods. Most effective geophysical methods for identifying (individual) fractures and/or fracture zones (a dense set of fractures) include VLF-EM (e.g. [14]), VLF-R [15], VLF-EM-gradient [16], RMT [17], EM-34 [18], Electric Resistivity Tomography [19] [20] or geoelectric null-arrays [21] [22]. The resolution of these methods with the exclusion of the geoelectric ones is however smaller than it was required in the given study, where fractures were expected to be in even less than 4 - 5 m distance.

In small scale, geotechnical tools would be perfect for fracture mapping, but they provide only point-like information. These methods are expensive and their application is strongly limited by field conditions, such as topography, artificial constructions, landslide risk or vegetation, which make the access to the study area difficult or even impossible. The Pressure-Probe method [23] which is a simplified version of the geotechnical instruments and which avoids all their aforementioned deficiencies may be an economic solution for such problems.

Reference [24] could detect fractures by GPR, but with only 5 m resolution. The investigations carried out by [25] had at the same time very good resolution but they were carried out on a quarry wall, due to that the plateau above the cliff is covered with a conductive weathered layer, which drastically reduces the

penetration depth of the GPR method. In the study by [26] ground-penetrating radar and frequency-domain electromagnetic induction methods proved to be capable to detect discrete fracture and conduit features. In Kádárta area GPR measurements proved to be unsuccessful.

Reference [27] mapped fissure networks by Schlumberger and Dipole-dipole configurations under laboratory conditions. Reference [28] used three-dimensional ERT to record and display all the major vertical cracks (of cm size), which could have been visually observed at the surface of the clay model. Reference [29] studied 2 - 4 mm wide fissures in clay. In the above mentioned laboratory measurements the cracks reached the surface which is not the case in our study site. Reference [30] characterised fissures within a fine-grained landslide using ERT while [31] mapped desiccation cracks with two- , and three-dimensional ERT on a flood embankment. In a karstic environment [21] [22] mapped successfully dense fracture systems by the resistivity method, using geoelectric null arrays. Small scale ERT measurements aiming to map dense fracture systems in karstic environment are not known.

Although resistivity methods may be suitable for detecting and localising fractures, it is always very useful to apply multiple methods for the verification of results. For this reason a fast and effective method, the Pricking Probe Method (PriP) was applied. PriP can be regarded as a simplified version of the cone penetration tests [32]. The PriP was successfully applied previously in archaeological investigations [33] to localise structures such as walls or flooring at shallow depth. The first geological application of the PriP displayed the structure of the study area, which correlated perfectly with its main structural directions [34].

The aim of our investigation was to recognise the factorisation of the study site. Factorisation means all features related to the fractures and fractures zones of a site, namely position, width and fragmentation level of the fracture zones and position, significance and characteristic distance of the fractures. It is supposed to be closely connected to the sediment/air/water filled portion of the rock volume. Narrow highly fractured rock zones can be regarded as (individual) fractures. A well-known geophysical method, the ERT and a new method, the Pri-P were used. Their simultaneous application enabled the better interpretation of results and verified the applicability of the PriP method in hydrogeological investigations.

2. Site Description

The small village of Kádárta lies approximately 1 km northeast from the city of Veszprém, Hungary (**Figure 1**). A small waterworks can be found at the Northern edge of a large plateau made up of fractured dolomite. The waterworks of Kádárta supplied drinking water for the city of Veszpém since 1972. The nitrate concentration in springwater increased by 15 - 20 mg/l over the following decades to about 30 - 35 mg/l. As a consequence, the spring was excluded from

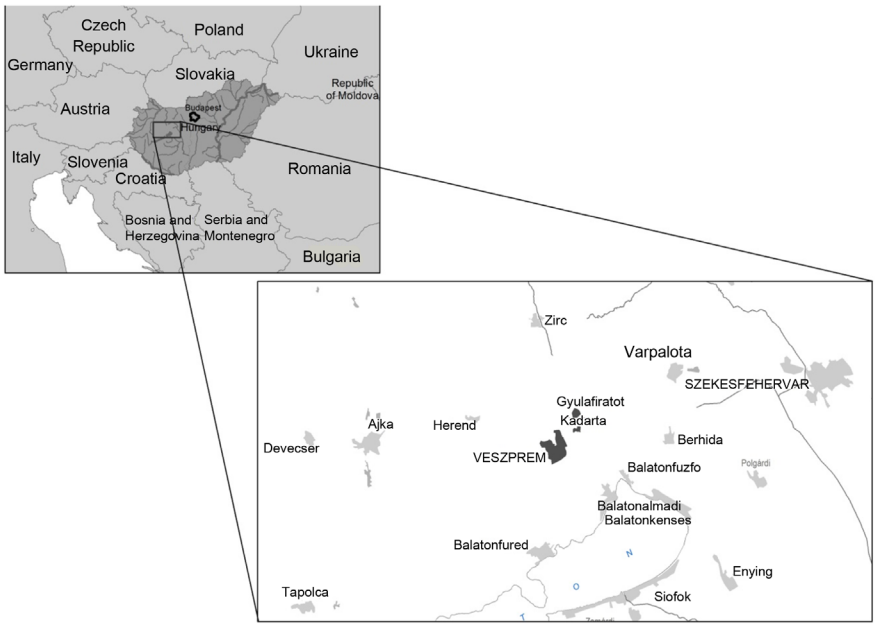

Figure 1. Location of the study area.

the drinking water distribution network. The study of [35] and [36] identified diffuse contamination, and concluded that nitrate originated from the application of fertilisers throughout the Veszprém plateau.

2.1. Geological Settings

The geological environment of the study area belongs to the Transdanubian Range which itself most probably is a result of the NW-SE compression of alpic nappes in the Cretaceous period and the subsequent extrusion of the Alcapa terrain from the late Oligocene to the Miocene. This entire mountain range can thus be described as an allochtonous structural element [37]. The Transdanubian Range as a whole can be interpreted as a series of succeeding thrust sheets.

The eastern part of the Veszprem plateau consists of NE-SW tending strips of upper-Triassic calcareous and clastic sediments, dipping 15˚ - 30˚ to the NW (**Figure 2**). The recurrence of these strips is a result of thrust faulting along two significant reverse fault lines in this area.

In a late eoalpian compression, N-S oriented strike-slip and normal faults developed, resulting in the presence of multiple faults [38]. The Kadarta springs are located along one of these traverse faults, which are indicated by dry valleys. The Kadarta aquifer consists of 1000 m thick, white, well stratified, middle-Triassic dolomite [39]. This aquifer is bordered by the sequence of underlying mid-Triassic low-permeability calcareous sediments from the SE, and overlying upper-Triassic marls from the NW. The Budaörs Dolomite pinches out to the SW in the area of Veszprémfajsz.

The dominant formation in the study area is the Budaörs Dolomite Formation (see BDF on **Figure 2**), which can be found in an elevated position, forming a

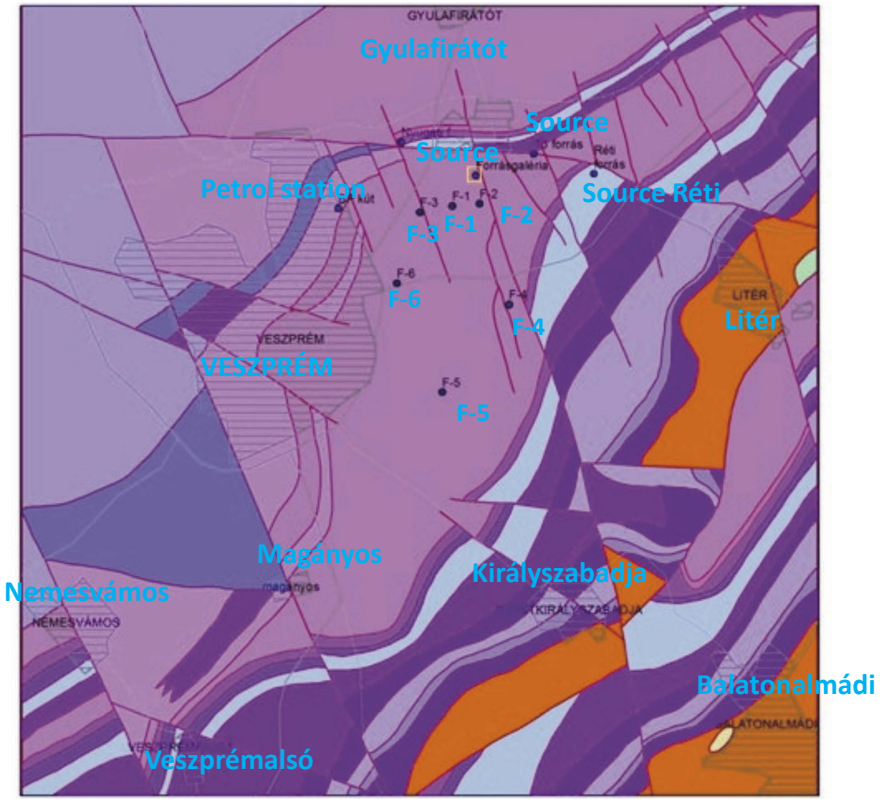

Figure 2. Geological settings of the Veszprém Plateau and vicinity. Kovács, 1998. *Yellow line rectangle*: study site with the main karst spring.

large plateau. This rock body mainly consists of highly fractured Triassic platform carbonates which prograded as a slope and toe-of-slope facies, and folded later in the Cretaceous due to NW-SE compression. The dimensions of this particular body of the BDF are approximately ten kilometres in length, two kilometres in width on the surface and could be 1000 metres deep at its thickest. Fracture zones in dolomite are profoundly significant in a hydrological respect, because of their high hydraulic conductivity mostly present in the so called "damage zone" of the ~10 - 15 m wide fractured zones [40].

The study area is at a structural boundary, where the plateau rises due to the Veszprém Thrust, a fault formed in the Cretaceous deformation phase, crossing the field in its southern part and resulting in high fracture density in many places. The exact interpretation of this structural element, however, is still unclear. It is either usually described as a thrust or a normal fault, as well as new theoretical models suggesting sections of it being an oblique ramp [41].

Dolomite surface is covered by 5 - 7 m thick quaternary loess in the SW, which is absent in the vicinity of the springs. The thin (10 - 20 cm) poor quality soils directly overlie the dolomite surface in this area.

2.2. Hydrogeological Settings

The catchment area of the springs is about 20 km^2. This area—as mentioned

above—has well defined topographical and geological borders. The waters, infiltrating through the dolomite, are drained by the Sed-stream and some karst springs, of which the Kadarta springs area the most significant. All the springs are located along N-S oriented valleys (which indicate traverse faults), at the contact of the aquifer and low permeability formations. The hydraulic gradient is about 10 - 12 m/km, having a direction of S-SW. The Kadarta-springs consist of two springs (western and eastern spring), located on both sides of the bottom of the valley, 100 meters away from each other. The total discharge of the Kadarta springs is about 8 - 11,000 m^3/day. A numerical groundwater flow model was constructed by [35] which outlined the recharge area of the springs. According to the model, average travel time is between 20 - 30 years in the Veszprém plateau area.

From a hydrogeological point of view, the role of this line is that it separates the hydraulically conductive Triassic BDF from aquicludes like the Veszprém Shale Formation, overlain by Iszkahegy Limestone, which form successive strata as part of a thrust sheet. This means that the Veszprém thrust itself can be determined as structural boundary between the nappes.

A large valley running into the ramp caused by the thrust can also be seen inside the area. The geological map of [42] indicates several parallel conductive fracture zones (**Figure 2**), corresponding to this valley well and other parallel trenches nearby.

2.3. Position of the Measuring Profiles

Both the ERT and PriP measurements were conducted on 4 parallel profiles (labelled P1 to P4 in **Figure 3(a)**, **Figure 3(b)**). The direction of the parallel profiles was nearly N-S and they were adapted to the shape of the fenced area. The position of the profiles is presented also on the topographical map of the site (**Figure 3(c)**).

3. Methods

3.1. Electrical Resistivity Tomography (ERT)

The electrical Resistivity Tomography (ERT) is one of the most often applied geophysical techniques for shallow subsurface investigations among others due to the fact that the electric resistivity of the rocks varies in a very wide range enabling the separation of different rocks. Since electrical resistivity depends strongly also on the water content of a rock, this method can be very successfully applied also in hydrogeological studies [43].

In this study Wenner-Schlumberger (W-S) configuration has been used. Reference [44] stated that the W-S array is the most sensitive configuration to detect changes in vertical resistivity and more sensitive than some other arrays (such as the Wenner) to the horizontal resistivity changes. Its great number of data points and extensive horizontal coverage [29] also justified its application. Its robustness may be also very important in a variable environment.

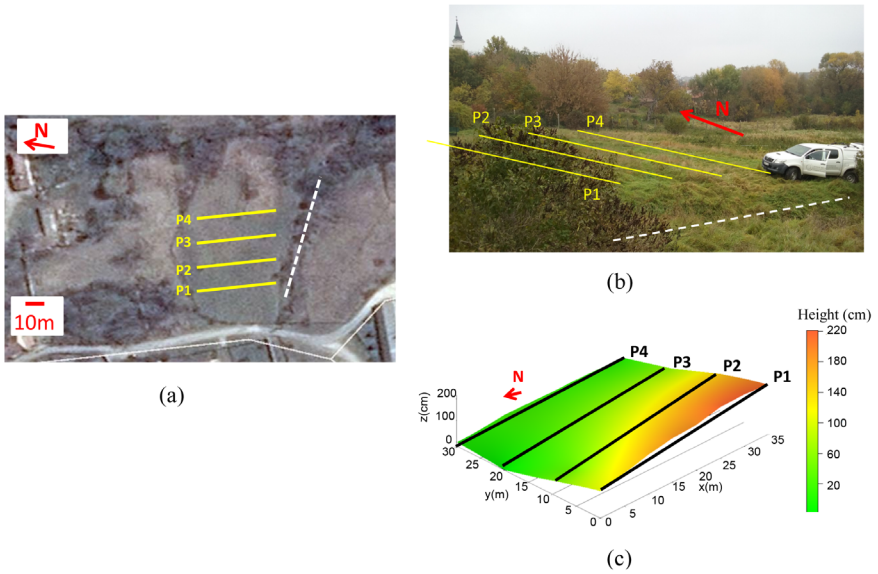

Figure 3. Position of the profiles: (a) on the aerial photograph; (b) on the photo of the study site; (c) on the topographic map of the site. The *white dotted line* presents the main fault line.

In the field measurement a 72 electrode Syscal Pro Standard & Switch system was used with 0.5 m electrode spacing. This configuration is able to give an image up to 7.2 m depth. 1010 data points were used for the deep and 695 data points for the shallow W-S section.

The measured values have to be inverted to obtain a resistivity section which can be interpreted for hydrogeological purposes. The inversion was done using Earthlmager 2D Version 2.1.7 [45]. In the resistivity inversion settings, the stop criteria were set with 3% RMS error and 5% error reduction, because 3% noise level was assumed in the field taking into account that the measurements have been carried out in a village. The inversion terminates on meeting one of the criteria in these settings.

In the inversion of the field data L1-norm did not produce better results than L2-norm not even in the shallow sections (**Figure 8**, **Figure 9**) which aimed to detect fractures. For this reason, all data were inverted using the L2-norm. Damping factor 1 was found to be the best. The RMS value which describes the fitting of the measured data and those calculated from the inverted model proved to be reasonable for all inversions without removing data.

To be able to detect fractures by the ERT method their electric resistivity values have to be different from that of the host rock. If the cracks in a dolomitic host rock are filled with clay or water, this criteria is satisfied, since their resistivity is less than 20 Ω·m contrary to the several thousands of Ω·m of the dolomite. In case of air-filled fractures the resistivity is very large. This strong variability of fracture resistivity can be confusing in the interpretation especially if the fractures are close to each other. Although water saturation could be estimated using factor analysis of engineering geophysical sounding data [46] we neglected it

both due to economical and ecological reasons. Measurements were undertaken following a rainy period to assure that the fractures were still almost completely water filled that is they were conductive.

3.2. Pricking Probe (PriP)

The Pricking Probe method was earlier only used for archaeological exploration purposes [33]. Its principle is demonstrated in **Figure 4**. A T-shape metal rod with a sharp peak is pushed into the soil into a given depth equidistantly along a profile. If the rod cannot reach the given depth due to that it sticks in a rock a k value 1, if it is able to reach it a value 0 will be assigned to the given position.

Due to that samples are only taken at given locations there is certain randomness in the results. To decrease it a running average of a certain number of consecutive measurements used to be displayed integrating in this way the effect of the volume between the first and last measuring points. 5 - 7 values seem to be practical to take into account in this process. The values determined in this way are called k_5 and k_7 and they are in the domain 0 to 1.

Figure 5 presents schematically the principle of the PriP. It was constructed using **Figure 2(b)** and **Figure 3** in Williams [47] and the cross-section obtained by Stewart and Parker [48] which demonstrates that the surfaces of the weathered and that of the fresh bedrock may be considered as parallel. This feature was also demonstrated indirectly by the downwards increasing GPR velocity values in [26].

Figure 5(c) presents differently weathered non-horizontal layers separated by blue curves. On the basis of the aforementioned papers, their boundaries are expected to be nearly parallel to each other and to the surface of the unweathered

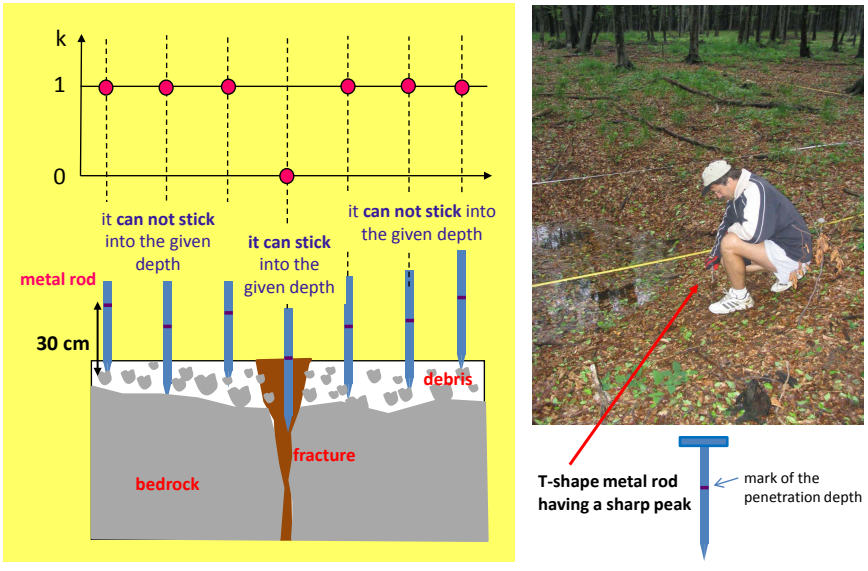

Figure 4. Performance of the PriP method. (a) Scheme of its operation and data presentation; (b) Its field application.

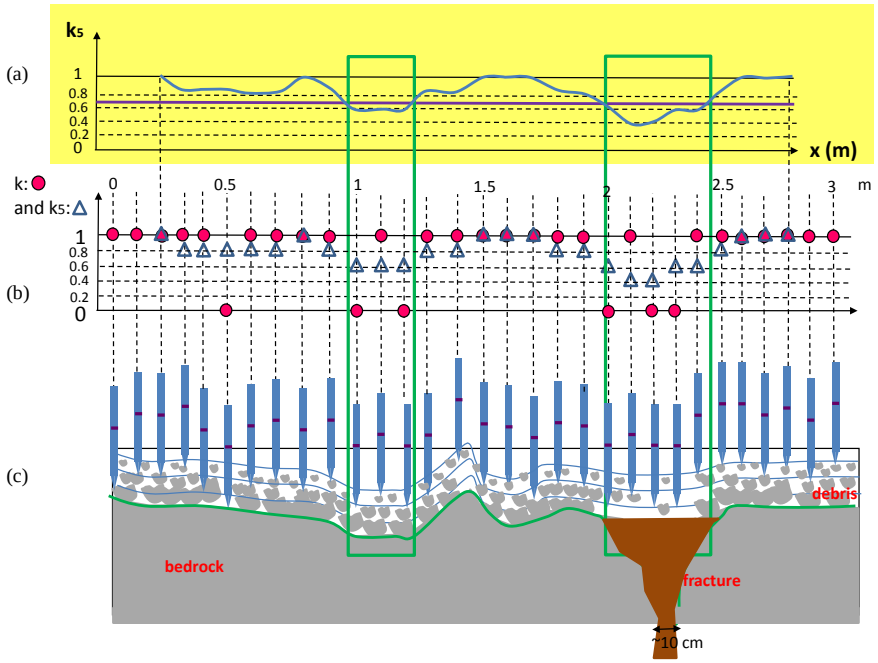

Figure 5. Schema of the mechanism of the PriP. (a) k_5 line; (b) k and k_5 values denoted by *red circles* and *blue triangles*, respectively; (c) Principle of the PriP method. *Blue curves* separate the differently wheathered rock domains. *Grey dots* represent the debris. *Green curve:* bedrock surface.

bedrock (denoted by thick green curve). The average size and the volume of the debris of the successive, equally thick "layers" approaching the surface are expected to be smaller and smaller due to the increasing weathering. With (decreasing debris volume, that is) increasing debris-free volume the probability that the Pressure Probe penetrates into the soil increases. Consequently k_5 or k_7 decreases with increasing distance from the bedrock.

Dissolution is more intensive close to a fracture because it serves as water flow path. Therefore also in the vicinity of a fracture the debris-free volume and thus the penetration probability must be larger than elsewhere. These areas are usually substantially wider than the fractures. In this way PriP method points to the existence of a fracture in a zone wider than the width of the fracture, enabling the application of a relatively great sampling distance. It also means that even rather narrow fractures may be detectable due to this effect.

The same was the situation in the study by [23] where the Pressure Probe method was applied, which is very similar to the PriP. In that study to detect fractures in loess it was definitely enough to apply a sampling distance three times the fracture width. Regarding the much larger consistency of the dolomite, the diameter of a valley due to a fracture may be much larger than the fracture width. A much weaker requirement is therefore enough for the sampling distance.

The diameter of the (often hidden) valley due to a fracture is the function in the first line the fracture width, dissolution capacity of the rock, dissolution time

and average rainfall quantity. It is worth to note that sampling distance can be almost optionally decreased, arbitrarily improving the resolution of the PriP method. Our field measurements themselves verified (see later in the interpretation of profiles P1 and P2) that the resolution of the PriP is not weaker than that of the ERT method, if the circumstances are convenient.

"Measured" k and k_5 values are presented in **Figure 5(b)**. Due to the randomness also at x = 0.5 m $k = 0$ value was taken, even if its probability is rather small. In zone x = 1 - 1.2 m two $k = 0$ values were taken because the rode penetrates here into intensively weathered rock. The same is the situation in the vicinity of the fracture. k_5 values were then calculated (presented by triangles in **Figure 5(b)**) and their connecting line was displayed in **Figure 5(a)**. Taking a threshold value of $k_5 = 0.7$, the zones x = 0.95 - 1.25 m and 2 - 2.45 m are delineated (**Figure 5(a)**). Severely weathered zones are supposed to be there. As it is seen, they correlate well with the depressions of the bedrock and depressions used to develop due to fractures. The appropriate choice of the threshold value requires field practice. It is well seen that the 0 value at 0.5 m did not influence significantly the result.

On the basis of this scheme it seemed to be possible to map the topography of the unweathered bedrock. Since dolomite is thought to be everywhere inside the study site, depressions in the bedrock surface must develop due to fractures and fracture zones. In this way fractures and fracture zones were expected to detect (indirectly) by the application of the PriP method.

0.3 m penetration depth and 0.1 m sampling rate are often well applicable PriP parameters. The best penetration depth can however be chosen with a trial measurement in the given area. Applying different penetration depths along the same profile that depth is regarded the best which produces the largest variability. If at least one fourth, but less than three forth of the values are 1, the method is most likely well applicable. Not far from the study area the 0.3 m penetration depth was completely useless, because all measured values were 1 that is it was not possible to stick the rod into 0.3 m depth anywhere. Using however 0.1 m penetration depth the method proved to be applicable. In the given study area the standard parameters were used since they proved to be perfect.

We assumed the existence of fractures, where k_5: 1. was below 0.2; 2. had a strong local minimum; 3. had a strong contrast in adjacent zones (see e.g. zones a, b and c in **Figure 8(b)**). In situations 1 and 2 the probability that the probe hits rocks is smaller due to that they are filled with fine sediments. In case 3 the alteration must occur due to sharp change in the depth of the bedrock that is by a fault, which also refers to the existence of a fracture. It means that all of these features most likely correspond to fractures.

The application of the PriP method is favourable because its application is very simple and it can be used even among the worst field conditions (extreme topography, weather). It is able to provide information also about the edges of the study area which may not be seen by ERT.

4. Major Sources of ERT and PriP Data Errors

Theoretically both methods should be able to detect fracture zones and even individual fractures. ERT measurements may produce convenient results if the electrical resistivity of the filling material of the fractures has a sufficiently large contrast with that of the dolomite and the distance of these features is sufficiently large in comparison to their depth. To get acceptable PriP results its sampling rate has to be small enough to get data from the fractures or their sufficiently eroded environment.

Even if the situation is theoretically convenient for the measurements, due to different noises the interpretation of the results may not be evident. Because resistivity is connected to fracture properties through water saturation it is recommended to carry out the measurements after a rainy period, when all fractures are more likely filled by water that is electrically more conductive than the host rock. In this way interpretation may be much easier. But even the results measured after a rainy period depend on many parameters (time of rainfall and its quantity before the measurements, water infiltration velocity, thickness of the cover, etc.) which also may make the ERT interpretation more complicated. The assumption, that the measurements are two-dimensional, are also often far to be valid. Among others fractures are rarely linear and there are present often also fractures orientated in other directions.

Due to the ambiguities of the ERT results it is recommended to verify them applying another method. The resolution of the VLF technique is weaker than required and GPR measurements could neither produce feasible results in the study site. Hence we decided to test the PriP method. It was its first verified geological application.

PriP data are affected by noise most often due to plants with thick roots which are also able to deny the probe to get into the required penetration depth. Since such plants can however be seen it is not difficult to treat the errors they produce. In our case there were not any such plants thus this kind of problem was irrelevant. Hollows of animal origin could also distort PriP results, but they did not occur in a large number and k averaging diminishes their effect rather well owing to their small extension similarly to the situation which was presented at x = 0.5 m in **Figure 5**. Human activity can however severely influence the PriP results by reorganizing the near-surface debris distribution. Building operation or agricultural activity may be the main causes of such distortions. In the study area artificial disturbances could only origin from building operations in the eastern part of the measure area. Their remnants may still be present in the area.

Positioning errors are misleading for both methods. It may not be as a serious problem measuring with one of the methods, but it is, if the aim is comparing the results of both techniques, especially if fracture density is high. In this case it is difficult to know whether a smaller shift between the anomalies of both methods is due to positioning errors or due to any other reason.

5. Field Results and Discussion

5.1. ERT Results 1: Overview Image

First of all the ERT sections are shown which served as a basis for all interpretations. P1 ERT section in Figure 6 does not display soil. It must be very thin. In zone 0 - 12 m (in horizontal direction) the uppermost layer is about 2 m thick with a resistivity value above 100 Ω·m. This layer is divided into highly resistive blocks in this zone, which are separated by thin lower resistivity zones. The latter are supposed to be sediment and/or water filled fractures. In spite of that the whole study area consists of dolomite the resistivity is about 50 Ω·m below this layer. Such a small resistivity value can only occur if the dolomite is fully saturated. Therefore the top of this small resistivity domain, in 2 m depth, appoints the karstwater level below P1 (shown by blue line in Figure 6). Other smaller resistivity green areas which reach close to the surface (~50 Ω·m at 12 - 20 m and 24 - 29 m) show that these areas are fractured also at a very shallow depth and saturated with water originating from rain fallen just before the measurements were undertaken. Zone 12 - 20 m seems to be the most suitable for water extraction as this zone has the smallest resistivity value (~20 Ω·m). Zone 20 - 24 m refers to a compact dolomite zone. At about 20 m there must be a fault according to this section.

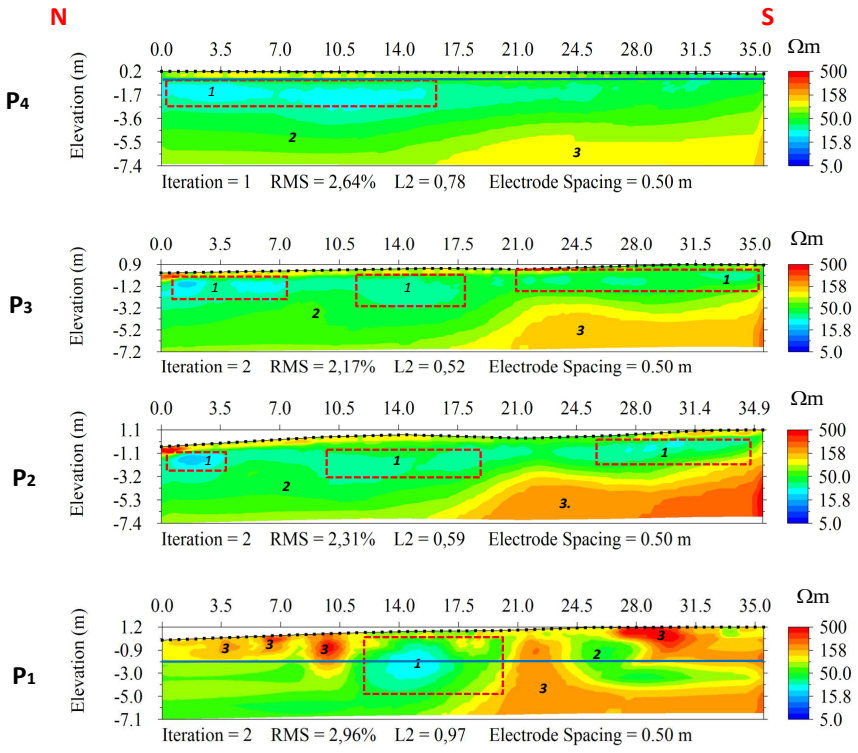

Figure 6. Deep ERT sections. *Numbers* denote resistivity areas which are interpreted as: (1) fractured dolomite (<30 Ω·m); (2) less fractured dolomite (30 - 100 Ω·m); (3) compact dolomite (>100 Ω·m). Zones 1 are delineated by *dotted line rectangles*. Blue line presents the supposed karstwater level.

The basis of the interpretation of the other profiles is similar. Numbers 1, 2, 3 in Figure 6 are supposed to denote the most, medium and less fractured zones, respectively, according to their increasing resistivity values. The less fractured zones correspond to very compact formations which do not let water through. The most remarkable difference among the profiles is that the surface of the highly resistive massive dolomite (at 20 - 35 m) deepens eastwards, from P1 to P4. The karstwater level (the upper edge of the blue colour areas) increases in the same direction being not deeper than 0.5 - 1 m below P4.

Although resistivity cannot be directly transformed to fracturing, because the water saturation of the near surface units is unknown, resistivity map may provide an acceptable image about the fracture zones of the study area. The map in Figure 7 was constructed from the shallowest values of the resistivity sections. The decreasing resistivity towards P4 is unambiguous. It probably refers to the increasing sediment and/or water content which may occur due to higher fracturing. The most remarkable feature in the map is the about W-E oriented small-resistivity "trench" which starts from x = 12 - 20 m in P1. It is interpreted to indicate zones with the highest water content corresponding to the most fractured part of the area. The direction of the trench is almost the same as that of the large fault which is 20 m right from this structure (Figure 3(a)).

It was shown that ERT can give a good image about the fracture zones. Now it will be discussed whether it is able to give a more precise image that is it can also detect individual fractures. This ability of the ERT will be compared to the one of the PriP method.

5.2. ERT Results 2: Detailed Image and Its Comparison with the Pricking Probe Results

We are going to study the shallowest ERT values in about 0.5 m depth (marked

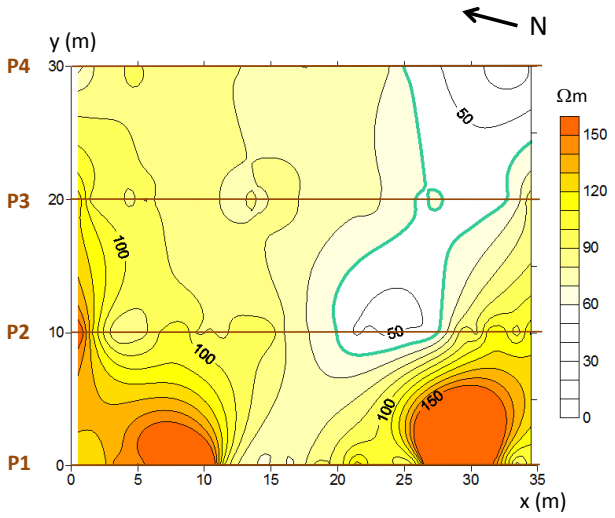

Figure 7. Resistivity distribution map displaying the shallowest ERT data.

by a white curve in Figure 8(a)), which are close to the investigation depth of the PriP. It enables the comparison of the results obtained by both methods. Resistivity variation must be due to the changes in the weathering level of the rock regarding that the study site uniformly consists of dolomite. More weathered dolomite has smaller resistivity due to the higher sediment and/or water content. Three longer sections denoted *a*, *b* and *c* can be seen in Figure 8(a), whose resistivity values are remarkably different. As it has already been discussed zone *a* describes the highly fractured zone. Zone *c* must be a very compact dolomite, while in zone *b* the dolomite is moderately fractured. Narrow low resistivity zones, which are marked by ellipses, must be intensely dissolved, most likely due to fractures. Three such fractures are seen in Figure 8(a). The presented three fracture zones and the three fractures are the principal features visible in the resistivity section.

The PriP profile presents the same three zones as the ERT one. The average *k* level is remarkably different in these zones: it is 0.08, 0.25 and 0.92 in zones *a*, *b* and *c*, respectively, presenting the decreasing fracturing. The features which are supposed to be fractures are well seen also in the PriP profile. *k* provides 0 value in these locations (feature 1 and 2) or a strong local minima (feature 5). All of these features are at the same locations as the ones denoted by the ERT section. Also the two significant resistivity maxima appear almost at the same positions where the PriP ones (red arrows). Two remarkable *k* minima (features 3 and 4) have at the same time no pair in the ERT section. Regarding, however, that they are at both ends of the highly resistive zone *a*, they are most probably linked also to tectonic features.

It can be concluded from Figure 8 that both methods provided principally the same results. They delineated three differently fractured zones and three significant fractures. It verifies that both methods would be able even individually

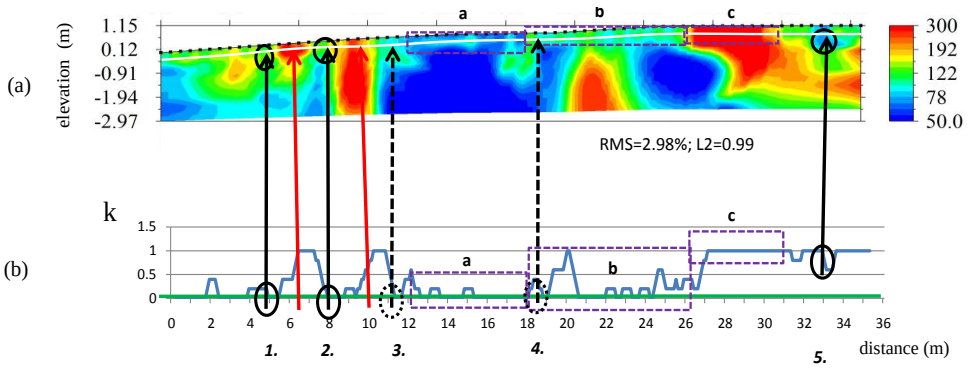

Figure 8. P1 field results. (a) Shallow ERT section; (b) Pricking-Probe results. *Green line* presents the $k = 0.2$ level. *White line* presents the depth from where the ERT values were taken to compare the results of both methods. The blocks where *k* is in about the same range are presented in *violet dotted line rectangles*. *Black arrows* display the supposed fracture positions on basis of the PriP results. They are *continuous if they* have their pair in the ERT section. Corresponding pairs are presented by *ellipses* in the ERT section. The *dotted line arrows* start from supposed PriP fractures which have not ERT pair. *Red arrows* connect the PriP and ERT maxima.

display such features. They can also verify each other's results which is also very important especially if results are very noisy.

The area along P3 (Figure 9) shows rather different characteristics. ERT displays a long fracture zone in 23 - 33 m, beside of six characteristic (denoted by continuous line ellipses) and nine not as characteristic (denoted by dotted line ellipses) fractures. The characteristic distance of the fractures is 1 - 1.5 m in the zones 2 - 7 m and 11 - 22 m. It is significantly smaller than the 3 m characteristic fracture distance which was observed along P1.

PriP results verify the existence of a fractured zone in 28 - 33 m (zone *c*), and all characteristic ERT fractures (denoted by continuous line ellipses) excluding only the 1st one. It verifies six of the eight fractures in zone 10 - 22 m, except only two not-remarkant fractures (the 9th and 11th ones). The shift in the positioning of these corresponding fractures is not more than 0.5 m which is reasonable especially regarding the possible positioning errors due to the field circumstances. *k* minima appeared again at both sides (at 23 and 34 m) of the ERT fracture zone.

In the 0 - 10 m and the 23 - 28 m zones at the same time the ERT and PriP values do not correlate. Due to that all along P1 there was a good correlation between the ERT and PriP values, we assume that the debris here are not natural origin or they were redisposed. Building remnants were found close to P4 which strengthen the possibility of human activity in this area. Probably building materials have been accumulated there covered by soil and vegetation resulting in misinterpretation of the PriP data.

Figure 9 highlights that there are still open questions regarding the applicability of the PriP method even if it produced very similar results to the ERT ones along 20 m from the 35 m. Human activity may especially strongly distort PriP results.

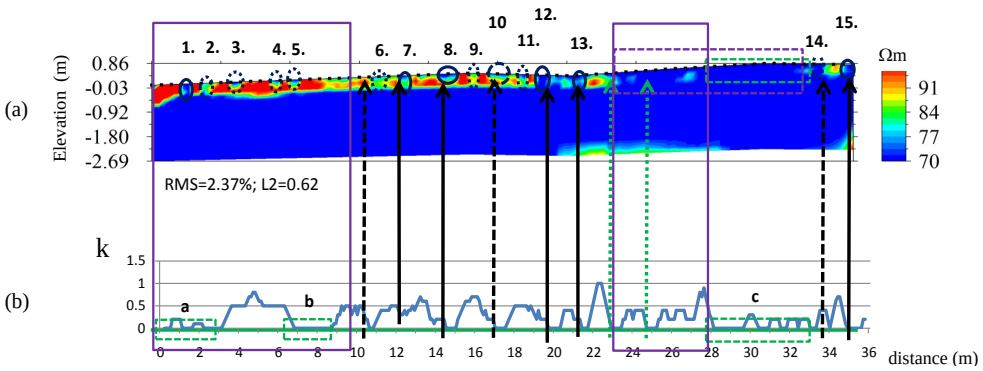

Figure 9. P3 field results. (a) Shallow ERT section; (b) Pricking-Probe results. *Green line* presents the $k = 0.2$ level. *Green dotted line rectangles* denote PriP fracture zones. *Lila dotted line rectangle*: ERT fracture zone. *Lila continuous line rectangle:* parts of the profile where the ERT-PriP correlation is bad. *Arrows*: supposed fracture positions on basis of the PriP results. *Continuous line ellipses:* more characteristic; dotted line ellipses: less characteristic ERT anomalies which may refer to fractures. Continuous *line arrows* connect well correlating ERT and PriP anomalies, *dotted line arrows* connect not as well correlating ones. *Green arrows* have no pair on the ERT section.

Fracturing map can be constructed using the PriP results, too (Figure 10). The displayed quantity is 1 − *k* in percent. Where there are no fractures *k* is 1 (fracturing is 0%), while where the rod is going into the soil without hitting a rock (that is there are not unweathered rock matrix elements) *k* is 0 (fracturing is 100%). The larger is the proportion of the unweathered rock matrix elements in a given volume the smaller is the probability that the rod can penetrate into the given depth, the larger is *k* and the smaller is the fracturing.

The PriP fracturing map (Figure 10) can be divided into three areas according to the fracturing level. Where there are the smallest values (zone *I*), the rock unit is very solid. Where are the largest values (zone *III*), the rock unit is strongly fractured. Zone *II* corresponds to a transition zone. Zone *IIIa* corresponds perfectly to the fault zone shown by the resistivity section in Figure 6 and Figure 8. It is questionable whether zone *IIIb* is also a fault zone. It must be noted that in the eastern part of the study site (y = 15 - 30 m, along P3 and P4) ERT and PriP results correlate poorly (as seen already discussing P3). In the western part (y = 0 - 15 m, along P1 and P2) however the correlation was good. The western part of the PriP and the ERT fracturing maps are very similar to each other.

While the PriP method was able to give a very good image in one part of the study site it was not able to do it in its other one. It verifies that this method is applicable to construct fracturing maps, but it has limitations which should still be further studied. This method proved however to be the only tool which could be applied to verificate the ERT results.

Correlation was also calculated between the PriP and the shallowest ERT curves. The values of the correlation coefficients are 0.59, 0.56, 0.13 and 0.07 for P1, P2, P3 and P4, respectively. The correlations for P1 and P2 are (in spite of

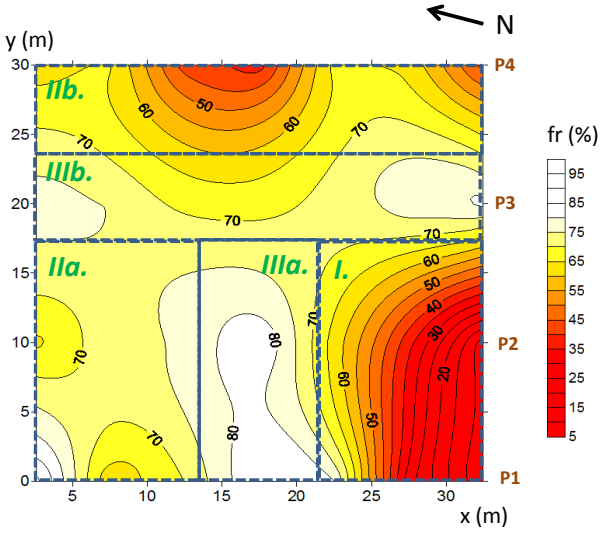

Figure 10. Fracturing map made on the basis of the *k* values. *Zones I-III.* correspond to different fracturing areas: *I.* massive dolomite; II. fractured dolomite; *III.* very fractured dolomite/ fault zone.

the underestimation due to among others the positioning errors) close to 0.6 showing that there is a significant relation between the ERT and PriP values. The P3 and P4 correlation values proved to be weak at the same time. The good correlation values in the western part (P1 and P2) of the area demonstrate again the applicability of the PriP method while the weak correlation in the eastern part (P3 and P4) verify the necessity of further studies to understand better the background of the method. The simplest and possible explanation would be human activity which modified the near-surface debris distribution. Wall remnants in the vicinity of P4 strengthen this explanation.

6. Conclusions

The aim of this study was to obtain information on the tectonic characteristics such as fracture patterns in a dolomite aquifer. Such information is indispensable e.g. in hydrogeological modelling. Beside the application of the Electrical Resistivity Tomography (ERT), the Pricking-Probe method has been tested, to see its applicability as an independent verification tool.

Beside of that, ERT produces information from greater depths supporting the interpretation of near-surface characteristics and the geology of the area, it can detect fractures, especially if the measurements are carried out following a rainy period and the distance between the fractures is large, in comparison with their depth. ERT results can also be used to construct porosity map, which is closely related to the fracturing one.

The PriP method is applicable to provide information about the subsurface conditions, when alterations manifest also near the surface. Since with increasing, fracturing the probe penetrates more likely into the desired depth, PriP is able to provide information about fracturing. Individual fractures can be regarded as very narrow zones with high fracturing. Since fractures are much wider at their top because the intensive dissolutions around them even narrow fractures are detectable with a reasonable sampling rate. Alterations in the *k* level may refer to faults.

Along one of the investigated profiles (P1), both methods provided principally the same results. They delineated three differently fractured zones and three significant fractures proving that both methods would be able to display such features even individually. They can therefore also verify each other's results which are also very important especially if data are heavily noise contaminated. Results along the other presented profile (P3) pointed however out that there are still open questions considering the applicability of the PriP method even if the highly fractured zone *c* is presented by both methods, and the position and the average distance of the supposed fractures in the middle of the profile proved also to be the same. Both methods could detect and localise even individual fractures in spite of their small distance.

The calculated correlation coefficients between the PriP and the shallowest ERT curves proved to be 0.59, 0.56, 0.13 and 0.07 for P1, P2, P3 and P4, respec-

tively. The good correlation values in the western part of the area (along P1 and P2) demonstrate the applicability of the PriP method, while the weak correlation in the eastern part (along P3 and P4) shows the necessity of further studies to better understand the background of the method. Weak correlation might be due to human activity which modified the near-surface debris distribution and consequently the PriP values.

The study demonstrates that the presented methods are able to describe the fracture patterns of an area. They are able to characterise both fracture zones and fractures. Such information is very useful e.g. for hydrogeologists and engineers.

In the study area, it was concluded that the surface of the unweathered dolomite is deepening both eastwards and northwards, similarly to the surface topography. A wide fracture zone was discovered on basis of the fracturing maps by both methods. This zone would be ideal for extracting water. A number of individual fractures have been localised in the west, in the moderately fractured areas at an average distance of about 3 m. In the eastern part of the site, in the highly fractured areas, there are more uncertainties, partly maybe due to the supposedly smaller 1 - 1.5 m fracture distance. This knowledge is principal in building hydrogeological models for the area.

ERT seems to be effective in describing the fracture pattern in spite of the uncertainties. To avoid the misinterpretation, further measurements with an independent method are recommended. Although its applicability and limitations have still to be studied PriP proved to be convenient for this aim. Furthermore, it may be the only applicable tool in small scale fracture studies close to the edges of the study site or in extreme field conditions, such as e.g. a very rugged terrain. The studied methods even individually can provide important information for hydrogeologists and engineers. Their joint application may even be more fruitful.

Acknowledgements

We would like to express our thanks to Csaba Molnár, Zsófia Zalai and Attila Hermann for their collaboration in the field survey and data processing. Special thanks to Attila Radács, the technical director of the Bakonykarszt Corporation and their colleagues to let us carry out the measurements in the study area.

References

[1] Karst in Europe COST 65 (1995) Hydrogeological Aspects of Groundwater Protection in Karstic Areas. Final Report COST Action 65), European Commission, Directorate General XII Science, Research and Development, Brussels, Report EUR 16547 EN, 446 p.

[2] Ford, D. and Williams, P.D. (2007) Karst Hydrogeology and Geomorphology. https://doi.org/10.1002/9781118684986

[3] Kaufmann, G. (2016) Modelling Karst Aquifer Evolution in Fractured, Porous Rocks. *Journal of Hydrology*, **543**, 796-807.

https://doi.org/10.1016/j.jhydrol.2016.10.049

[4] Mangin, A. (1975) Contribution à l'étude hydrodynamique des aquifères karstiques. Thèse, Université de Dijon, 124 p.

[5] Kiraly, L. (1975) Rapport sur l'état actuel des connaissances dans le domaines des caractères physiques des roches karstiques. In: Burger, A. and Dubertret, L., Eds., *Hydrogeology of Karstic Terrains*, International Union of Geological Sciences, Paris, B(3), 53-67.

[6] Drogue, C. (1980) Test for Identifying the Type of Structure of Carbonates Fissures' Storages. Application à l'interprétation de certains aspects du fonctionnement hydrogéologique. *Mémoires hors série Société Géologique de la France*, **11**, 101-108.

[7] Kovács, A. (2003) Geometry and Hydraulic Parameters of Karst Aquifers: A Hydrodynamic Modeling Approach. PhD Thesis, University of Neuchâtel, Neuchâtel (CH).

[8] Kovács, A., Perrochet, P., Király, L. and Jeannin, P.Y. (2005) A Quantitative Method for the Characterization of Karst Aquifers Based on Spring Hydrograph Analysis. *Journal of Hydrology*, **303**, 152-164. https://doi.org/10.1016/j.jhydrol.2004.08.023

[9] Le Borgne, T., Bour, O., Riley, M.S., Gouze, P., Pezard, A., Belghoul, A., Lods, G., Le Provost, R., Greswell, R.B., Ellis, P.A., Isakov, E. and Last, B.J. (2007) Comparison of Alternative Methodologies for Identifying and Characterizing Preferential Flow Paths in Heterogeneous Aquifers. *Journal of Hydrology*, **345**, 134-148. https://doi.org/10.1016/j.jhydrol.2007.07.007

[10] Szabó, N.P., Kormos, K. and Dobróka, M. (2015) Evaluation of Hydraulic Conductivity in Shallow Groundwater Formations: A Comparative Study of the Csókás' and Kozeny-Carman Model. *Acta Geodaetica et Geophysica*, **50**, 461-477. https://doi.org/10.1007/s40328-015-0105-9

[11] National Research Council (1996) Rock Fractures and Fluid Flow: Contemporary Understanding and Applications. The National Academies Press, Washington DC.

[12] Hernádi, B., Balla, B., Czesznak, L., Horányi-Csiszár, G., Sűrű, P. and Tóth, K. (2013) Felszíni és felszínalatti (barlangi és többrvizsgálatok) valamint a Bükki karsztvízszint észlelő rendszer (BKÉR) adatainak térinformatikai rendszerbe történő szervezése. A Magyar Hidrológiai Társaság XXXI. Országos Vándorgyűlése, Gödöllő.

[13] Kovács, A., Perrochet, P., Darabos, E., Lénárt, L. and Szűcs, P. (2015) Well Hydrograph Analysis for the Characterisation of Flow Dynamics and Conduit Network Geometry in a Karst Aquifer. Bükk Mountains, Hungary. *Journal of Hydrology*, **530**, 484-489. https://doi.org/10.1016/j.jhydrol.2015.09.058

[14] Rajaraman, H.S., Babu, V.R., Dandele, P.S., Chavan, S.J., Achar, K.K. and Babu, P.V.R. (2011) Using VLF-EM to Delineate a Fracture Zone in Basement Granites for Uranium Exploration. *The Leading Edge*, **30**, 1158-1162. https://doi.org/10.1190/1.3657076

[15] Kaikkonen, P., Sharma, S.P. and Mittal, S. (2012) 3D Modeling and Inversion of VLF and VLF-R Electromagnetic Data. *Geophysics*, **77**, 219-231. https://doi.org/10.1190/geo2011-0360.1

[16] Bosch, F.P. and Müller, I. (2005) Improved Karst Exploration by VLF-EM-Gradient Survey: Comparison with Other Geophysical Methods. *Near Surface Geophysics*, **3**, 299-310. https://doi.org/10.3997/1873-0604.2005025

[17] Turberg, P., Müller, I. and Flury, F. (1994) Hydrogeological Investigation of Porous Environments by Radio Magnetotelluric Resistivity (RMT 12-240 kHz). *Journal of*

Applied Geophysics, **31**, 133-143. https://doi.org/10.1016/0926-9851(94)90052-3

[18] Kellett, R. and Bauman, P. (2004) Mapping Groundwater in Regolith and Fractured Bedrock using Ground Geophysics: A Case Study from Malawi, SE Africa. *CSEG Recorder*, **29**, 25-33.

[19] Francese, R., Mazzarini, F., Bistacchi, A., Morelli, G., Pasquarè, G., Praticelli, N., Robain, H., Wardell, N. and Zaja, A. (2009) A Structural and Geophysical Approach to the Study of Fractured Aquifers in the Scansano-Magliano in Toscana Ridge, Southern Tuscany, Italy. *Hydrogeology Journal*, **17**, 1233-1246. https://doi.org/10.1007/s10040-009-0435-1

[20] McCormack, T., O'Connell, Y., Daly, E., Gill, L.W., Henry, T. and Perriquet, M. (2017) Characterisation of Karst Hydrogeology in Western Ireland using Geophysical and Hydraulic Modelling Techniques. *Journal of Hydrology Regional Studies*, **10**, 1-17. https://doi.org/10.1016/j.ejrh.2016.12.083

[21] Szalai, S., Szarka, L., Prácser, E., Bosch, F., Müller, I. and Turberg, P. (2002) Geoelectric Mapping of Near-Surface Karstic Fractures by Using Null-Arrays. *Geophysics*, **67**, 1769-1778. https://doi.org/10.1190/1.1527077

[22] Falco, P., Negro, F., Szalai, S. and Milnes, E. (2013) Fracture Characterisation using Geoelectric Null-Arrays. *Journal of Applied Geophysics*, **93**, 33-42. https://doi.org/10.1016/j.jappgeo.2013.03.005

[23] Szalai, S., Szokoli, K. and Metwaly, M. (2014) Delineation of Landslide Endangered Areas and Mapping Their Fracture Systems by the Pressure Probe Method. *Landslides*, **11**, 923-932. https://doi.org/10.1007/s10346-014-0509-6

[24] Barnhardt, W.A. and Kayen, R.E. (2000) Radar Structure of Earthquake-Induced, Coastal Landslides in Anchorage, Alaska. *Environmental Geosciences*, **7**, 38-45. https://doi.org/10.1046/j.1526-0984.2000.71007.x

[25] Jeannin, M., Garambois, S. and Jongmans, D.G. (2006) Multiconfiguration GPR Measurements for Geometric Fracture Characterization in Limestone Cliffs (Alps). *Geophysics*, **71**, 85-92. https://doi.org/10.1190/1.2194526

[26] Steelman, C.M., Kennedy, C. and Parker, B.L. (2015) Geophysical Conceptualization of a Fractured Sedimentary Bedrock Riverbed using Ground Penetrating Radar. *Journal of Hydrology*, **521**, 433-446. https://doi.org/10.1016/j.jhydrol.2014.12.001

[27] Jones, G., Zielinski, M. and Sentanac, P. (2012) Mapping Desiccation Fissures using 3-D Electrical Resistivity Tomography. *Journal of Applied Geophysics*, **84**, 39-51. https://doi.org/10.1016/j.jappgeo.2012.06.002

[28] Samouelian, A., Cousin, I., Richard, G., Tabbagh, A. and Bruand, A. (2003) Electrical Resistivity Imaging for Detecting Soil Cracking at the Centimetric Scale. *Soil Science Society of America Journal*, **67**, 1319-1326. https://doi.org/10.2136/sssaj2003.1319

[29] Sentenac, P. and Zielinski, Ć.M. (2009) Clay Fine Fissuring Monitoring using Miniature Geo-Electrical Resistivity Arrays. *Environmental Earth Sciences*, **59**, 205-214.

[30] Bievre, G., Jongmans, D., Winiarski, T. and Zumbo, V. (2012) Application of Geophysical Measurements for Assessing the Role of Fissures in Water Infiltration within a Clay Landslide (Trieves Area, French Alps). *Hydrological Processes*, **26**, 2128-2142. https://doi.org/10.1002/hyp.7986

[31] Jones, G., Sentanac, P. and Zielinski, M. (2014) Desiccation Cracking using 2-D and 3-D Electrical Resistivity Tomography: Validation on a Flood Embankment. *Journal of Applied Geophysics*, **106**, 196-211. https://doi.org/10.1016/j.jappgeo.2014.04.018

[32] van Maanen, P., Schokker, J., Harting, R. and de Bruijn, R. (2017) Nationwide Lithological Interpretation of Cone Penetration Tests using Neural Networks. *Geophysical Research Abstracts*, **19**, EGU2017-8473.

[33] Szalai, S., Lemperger, I., Pattantyús-Ábrahám, M. and Szarka, L. (2011) The Standardized Pricking Probe Surveying and Its Use in Archaeology. *Journal of Archaeological Science*, **38**, 175-182. https://doi.org/10.1016/j.jas.2010.09.002

[34] Szalai, S., Veress, M., Novák, A. and Szarka, L. (2008) Application of the Simplest Geophysical Method, the Pricking Probe Method to Map Bedrock Topography in a Karstic Area. *Near Surface Geophysics Conference*, Krakow, 15-17 September 2008, 17. https://doi.org/10.3997/2214-4609.20146303

[35] Kovács, K., Csepregi, A., Izápy, G. and Kun, E. (1998) Plan for Protection of Water-Reservoir of Kádárta for Veszprém City (in Hungarian). Research Report by VITUKI, Water Resources Research Centre Plc., Budapest.

[36] Kovács, A., Csepregi, A., Izápy, G. and Kun, E. (2001) The Effect of Agricultural Activity on the Water Quality of a Karstic Groundwater Supply near Veszprem, Hungary. *Proceedings of the* 3*rd International Conference on Future Groundwater Resources at Risk*, Lisbon, 25-27 June 2001, 381-389.

[37] Tari, G. and Horváth, F. (2010) Eo-Alpine Evolution of the Transdanubian Range in the Nappe System of the Eastern Alps: Revival of a 15 Years Old Tectonic Model. *Földtani Közlöny*, **140**, 483-510.

[38] Dudko, A. (1991) Structural Elements of the Balaton Area. MAFI, Budapest.

[39] Budai, T. and Csillag, G. (1995) Triassic Formations of the Bakony-Mountains and the Balaton Area. MAFI, Budapest.

[40] Bense, V.F., Gleeson, T., Loveless, S.E., Bour, O. and Scibek, J. (2013) Fault Zone Hydrogeology. *Earth-Science Reviews*, **127**, 171-192. (In Hungarian) https://doi.org/10.1016/j.earscirev.2013.09.008

[41] Csicsek, L.Á. (2015) The Position and Structural Evolution of the Veszprém Thrust in the Light of New Field Data (Veszprém Plateau, Hungary).

[42] Láng, G. (1962) Hydrogeological Atlas of Hungary. Magyar Állami Földtani Intézet, 52-54.

[43] Revil, A., Karaoulis, M., Johnson, T. and Kemna, A. (2012) Review: Some Low-Frequency Electrical Methods for Subsurface Characterization and Monitoring in Hydrogeology. *Hydrogeology Journal*, **20**, 617-658. https://doi.org/10.1007/s10040-011-0819-x

[44] Tabbagh, J., Samouelian, A. and Cousin, I. (2007) Numerical Modelling of Direct Current Electrical Resistivity for the Characterisation of Cracks in Soils. *Journal of Applied Geophysics*, **62**, 313-323. https://doi.org/10.1016/j.jappgeo.2007.01.004

[45] Advanced Geosciences, Inc. (2006) Resistivity and IP Inversion Software. Instruction Manual for Earth Imager 2D, Version 2.1.7.

[46] Szabó, N.P., Dobróka, M. and Drahos, D. (2012) Factor Analysis of Engineering Geophysical Sounding Data for Water Saturation Estimation in Shallow Formations. *Geophysics*, **77**, 35-44. https://doi.org/10.1190/geo2011-0265.1

[47] Williams, P.W. (2008) The Role of the Epikarst in Karst and Cave Hydrogeology: A Review. *International Journal of Speleology*, **37**, 1-10. https://doi.org/10.5038/1827-806X.37.1.1

[48] Stewart, M. and Parker, J. (1992) Localization and Seasonal Variation of Recharge in a Covered Karst Aquifer System. *International Contributions to Hydrogeology*, **13**, 443-460.